CFD-Based Comparative Study of Axe Bow and Bulbous Bow Designs for Corvette Warship Deployment in Natuna Waters

Yeddid Yonatan Eka Darma[1*], Reyhan Arfananda Sugiarto[2], Achdri Fauzi Nugraha Oloan[3], Fajri Narotama[4]
(Received: 2 August 2025 / Revised: 12 August 2025 /Accepted: 13 August 2025 / Available Online: 8 September 2025)

***Abstract*— The Natuna Sea is considered a prime maritime area for Indonesia, bearing strategic and defense significance, besides its turbulent sea conditions demand warships to adopt or be provided with efficient and stable hull forms. Thus, this study is intended to investigate the most appropriate bow designs for a corvette warship operating in the Natuna region. Three types of bow are compared: a conventional V-hull, sloped bow, bulbous bow and axe bow. Comparison through Computational Fluid Dynamics (CFD) simulation, validated with Holtrop and Savitsky empirical methods, at the speed of 30 knots. Principal dimensions of the corvette were obtained through regression analysis from 20 other warships that belong to the same class. Results reveal that the axe bow has the smallest resistance, that is, 365.18 kN from Holtrop method and 374.27 kN from CFD in contrast to 384.43 kN owing to conventional bow design. It also fulfills all criteria of operation performance and fuel efficiency. Hence, it is considered the best alternative for corvette deployment into the Natuna Sea.**

Keywords— CFD Analysis, Corvette Warship Design, Hull Performance, Ship Resistance

*Corresponding Author:yeddidyonatan@poliwangi.ac.id

I. INTRODUCTION

The Natuna Sea, which lies to the north within Indonesia's exclusive economic zone, is thus very critical for national maritime defence because of its geopolitics and economy [1]. It also suffers from dynamic and steep seas due to which operations on the naval vessels become troubled [2]. Thus, performance and stability in terms of operation within the area also need requirements in design, emphasizing hydrodynamic resistance as well as hull mode considerations for these warships [3][4].

In naval architecture, the design of the bow significantly influences a vessel's resistance characteristics and overall performance efficiency [5]. The various types of bows such as bulbous bow and axe bow have been incorporated for different kinds of ships so as to improve the seakeeping capabilities and reduce drag [6][7][8]. Much is said about the performance of these types of bows in various studies, however, very few if any, can be found in the literature that directly compares them through the application of Computational Fluid Dynamics (CFD) methods [9], specifically concerning small-to-medium classes of warships like corvette.

This study aims to contribute to this gap by conducting a CFD-based comparative analysis of axe and bulbous bow hull forms for a concept design corvette intended for deployment in the Natuna Sea. Accordingly, it is hoped that the outcoming results will contribute to the selection of the hull, which will offer the best operational performance, propulsion efficiency, and reduced fuel consumption in difficult marine scenarios.

II. METHOD

A. Principal Dimension Estimation

In the present study, the principal dimensions of the corvette warship were determined statistically using linear regression [10]. Data collected from various reference naval vessels for comparison were then used in regression analysis to compute the dimensions of the target ship. The procedure began with the construction of a graph with the vessel service speed (V_s) on the x-axis and the key ship dimensions of length, beam, and draft on the y-axis. The graphical analysis thus revealed proportional relationships between V_s and the main dimensions.

The linear regression analysis was conducted using data from 20 corvette-class warships worldwide that are suitable for the Natuna coastal environment, with data sourced from publicly accessible online databases. The analysis produced estimated principal dimensions for the conceptual corvette design, resulting in a length overall (LOA) of 68.75 m, a beam (B) of 8.51 m, and a draft (T) of 2.90 m. For simplification and design standardization, these values were rounded to 69 m (LOA), 8.5 m (B), and 2.9 m (T). The service speed (V_s) selected for the vessel

Yeddid Yonatan Eka Darma is with Study Program of Ship Manufacturing Engineering, Politeknik Negeri Banyuwangi, Banyuwangi, 68461, Indonesia, and the Department of Ocean Engineering, Institut Teknologi Sepuluh Nopember, Surabaya, 60111, Indonesia. e-mail: yeddidyonatan@poliwangi.ac.id
Reyhan Arfananda Sugiarto is with Study Program of Ship Manufacturing Engineering, Politeknik Negeri Banyuwangi, Banyuwangi, 68461, Indonesia. e-mail: reyhanarfa67@gmail.com
Achdri Fauzi Nugraha Oloan is with Study Program of Ship Manufacturing Engineering, Politeknik Negeri Banyuwangi, Banyuwangi, 68461, Indonesia. e-mail: achdri@poliwangi.ac.id
Fajri Narotama is with the Indonesian Navy as an Engineer and Submarine Diving Officer, Surabaya, 60155, Indonesia. e-mail: narotamakaigun@gmail.com

is 30 knots, in line with operational requirements and comparative vessel capabilities.

The initial hull form development was based on this regression information. The first hull modeled was of the V-type shape, which was subsequently altered into three bow variations: sloped bow, bulbous bow, and axe bow, for the study of their hydrodynamic resistance performance.

B. Conceptual Hull Shape Design

The hull modeling process commenced after determining the vessel's principal dimensions through linear regression analysis. A V-type hull was selected for the preliminary design and initially drafted using 2D CAD software such as AutoCAD.

The design refers to the standards outlined by Lloyd's Register [11], which specify a girth chine location of 500 mm and a maximum deadrise angle of 30°. The Rule Length, defined as the distance along the design waterline from the forward perpendicular (FP) to the aft end of the rudder post (AP), was calculated to be 63.72 meters for this vessel [11].

For the bow region, the initial deadrise angle was set at 37°, based on guidance from The Ultimate Guide to the Traditional Deep V Boat. The stern configuration was designed according to Ship Design: Methodologies of Preliminary Design, reflecting the characteristics of a naval vessel, consistent with the vessel type considered in this study [12]. The resulting hull geometry, which complies with these criteria, is illustrated in Figure 1.

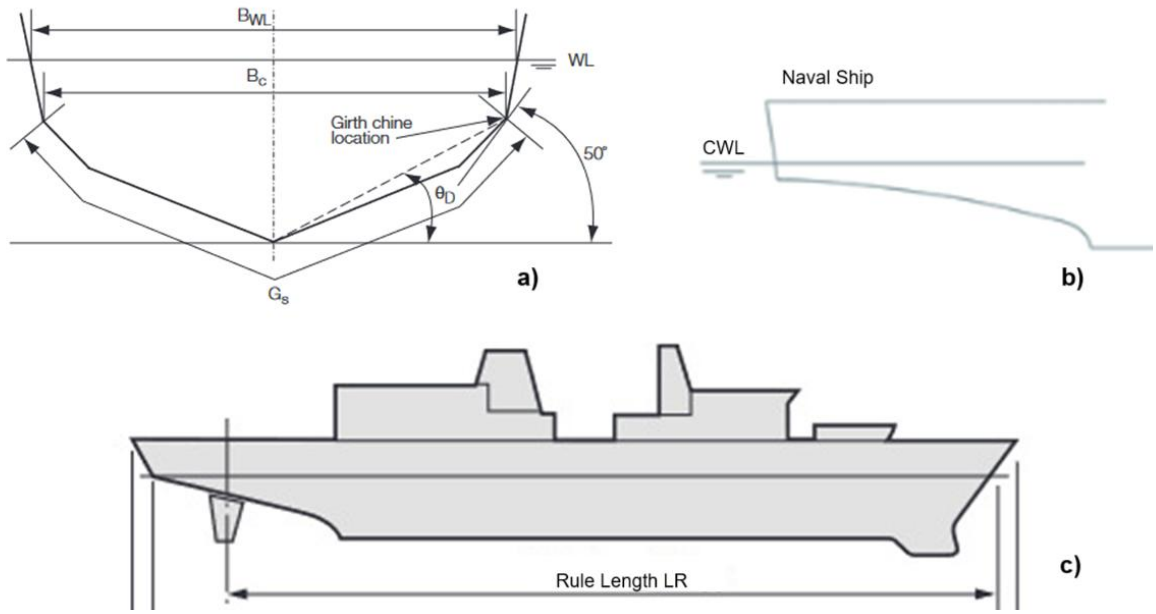

Figure. 1. V-Type Hull Form Design Overview: (a) LR Regulations on V-Hull, (b) Stern Configuration Based on Preliminary Ship Design Methodologies, (c) Rule Length Based on Lloyd's Register [11][12].

Two bow forms were selected this study, the bulbous and the axe bow. These were applied by modifying the initial hull sketch to incorporate each bow type, based on calculated parameters.

The bulbous bow was developed using established equations to determine its geometry. To enable the use of that bulbous-bow geometry, the following coefficients were used to establish the other parameters: the breadth coefficient (C_{BB}), the length coefficient (C_{LPR}), and the height coefficient (C_{ZB}) [13]. These coefficients are defined as follows:

$$C_{BB} = \frac{B_B}{B};\ C_{LPR} = \frac{L_{PR}}{L_{PP}};\ C_{ZB} = \frac{Z_B}{T_{FT}} \quad (1)$$

where B_B is the breadth of the bulb, B is the ship's breadth, L_{PR} is the longitudinal length of the bulb, L_{PP} is the length between perpendiculars, Z_B is the vertical height of the bulb, and T_{FT} is the draft to the flat of the bottom.

Based on the design data (principal dimensions of the ship), the coefficient values obtained were as follows: C_{BB} equals to 0.19; C_{LPR} equals to 0.026; and C_{ZB} equals to 0.48. These values were compared with the recommended limits presented in the reference by Kracht, Design of Bulbous Bow, which specifies that the permissible ranges for these coefficients are 0.17 to 0.20 for C_{BB}, 0.018 to 0.031 for C_{LPR}, and 0.26 to 0.55 for C_{ZB} [13].

All the computed coefficient values fall within their respective recommended ranges, indicating that the proposed bulbous bow dimensions conform to accepted design criteria. As a result, the bulbous bow model was developed using these calculated dimensions (Figure 2).

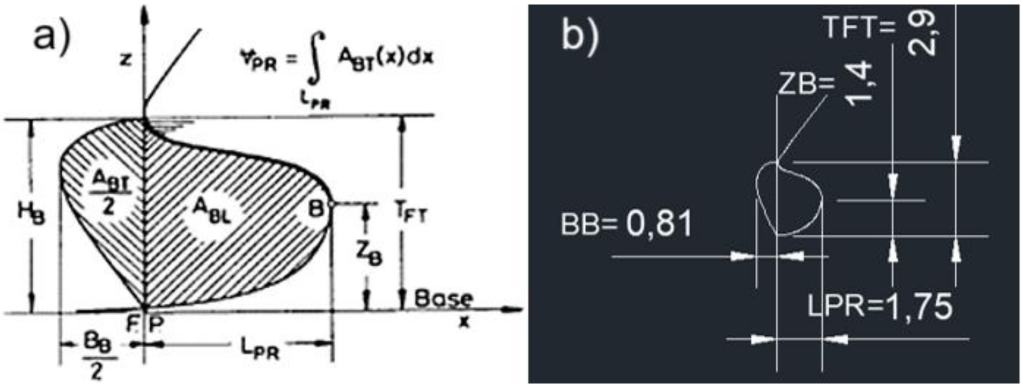

Figure. 2. (a) Geometric Parameters and Cross-Sectional Profile of a Bulbous Bow, (b) The Corresponding Design of the Bulbous Bow Model [13].

Following the dimensional design and evaluation of the bulbous bow configuration, the study proceeded to the investigation of the Axe Bow design, which presents a novel alternative for enhancement of hydrodynamic performance, especially while in rough seas. For the depth configuration of the Axe Bow, three design variations were considered, as represented in Figure 3, which amounts to 30%, 40%, and 50% of the design draft of the vessel. The 50% depth configuration emerged from resistance evaluations as the most favorable option in minimizing resistance. In agreement with this, Aulia and Adi [14] stated that when the hull form of the Axe Bow is adapted for patrol vessels, a similar modification to the resistance behavior is observable. The depth configuration was calculated using the following formula:

$$Depth\ Configuration = 50\% \times T \quad (2)$$

where T is the draft of the ship [14].

For this reason, 50% of the total draft (T) was taken as the Axe Bow depth, which gave a value of 1.45 m from a draft (T) of 2.9 m.

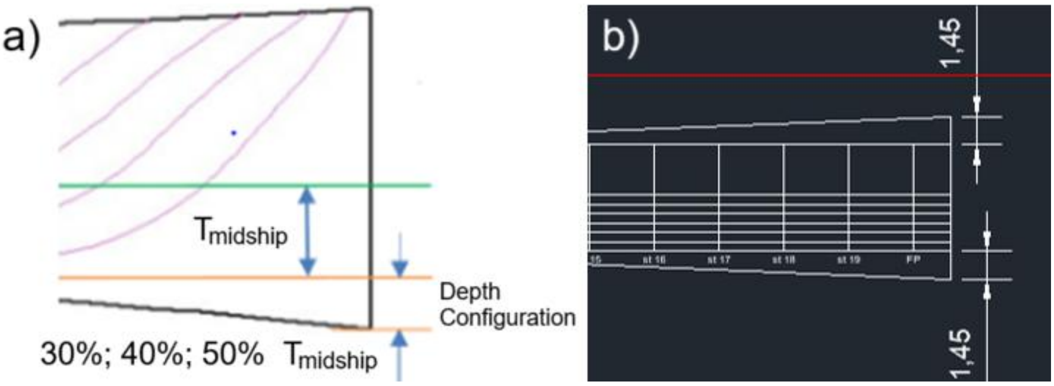

Figure. 3. (a) Schematic Representation of Depth Configuration, (b) Implementation of the Selected 50% draft.

This dimension was then imposed to the Axe Bow and Bulbos Bow geometry for application in the following computation modeling and resistance simulation.

C. Resistance Analysis with CFD

Understanding ship resistance is essential in evaluating hull performance and developing reliable resistance predictions. Ship resistance is defined as the hydrodynamic force that acts in opposition to a vessel's motion through water. This resistance primarily results from the interaction between the hull surface and the surrounding fluid [15]. A major component of this force is viscous resistance, which includes frictional resistance caused by shear stress between the water and the hull surface, as well as form resistance that arises due to the geometric characteristics of the hull (Savitsky method). The total resistance (R_T) acting on a vessel can be calculated using the following expression:

$$R_T = C_T \times \frac{1}{2} \times \rho \times v_s{}^2 \times S \quad (3)$$

where C_T is the total coefficient of resistance, ρ is sea water density (kg/m³), V_s is the ship's service speed (m/s), and S is wetted surface area (m²) [16].

To evaluate these resistance components with greater detail and adaptability across various operating conditions, calculation methods such as CFD are used. CFD enables numerical simulations of fluid flow around the hull, providing insight into hydrodynamic behavior and supporting performance analysis [17].

CFD operates by numerically solving fluid flow equations within a defined computational domain. This involves discretizing the geometry into a mesh and applying governing equations such as the continuity and Navier–Stokes equations. For incompressible flows, the Navier–Stokes equations and the continuity equation, which ensures mass conservation over time, can be mathematically represented as follows [18][19][20]:

$$\frac{\partial u_i}{\partial x_i} = 0 \tag{4}$$

where U_i is the time-averaged velocity components in Cartesian directions, and X_i is the Cartesian coordinates.

$$\frac{\partial u_i}{\partial t} + \frac{\partial (u_i u_j + \overline{u'_i u'_j})}{\partial x_j} = R_i - \frac{1}{\rho}\frac{\partial p}{\partial x_i} + \frac{\partial}{\partial x_j}\left(v\left(\frac{\partial u_i}{\partial x_j} + \frac{\partial u_j}{\partial x_i}\right)\right) \tag{5}$$

$$v = \frac{\mu}{\rho} \tag{6}$$

where t is time, R_i is the volume force, P is the time average pressure, v is kinematic viscosity, μ is dynamic viscosity, ρ is the density of water.

CFD is practical, as compared to physical testing of such models; for example, one can make multiple simulations by varying any parameter and still get accurate results [21]. In this study, the hydrodynamic characteristics of different hull designs were evaluated using CFD, while the hull-fluid interaction was computed.

The first step is three-dimensional hull modeling, followed by mesh generation and setting the boundary condition definition including boundary conditions used in this simulation as illustrated in Figure 4. For the computational domain, the boundary parameters are defined relative to the ship's Length Between Perpendiculars (*LPP*), which is the distance measured along the waterline from the (*FP*) forward perpendicular (typically at the intersection of the stem and the design waterline) to the (*AP*) aft perpendicular (usually at the rudder post or stern). In this simulation, the upstream boundary is positioned at a distance equal to 3 × *LPP* from the bow, while the downstream boundary extends 0.5 × *LPP* beyond the stern. The vertical and lateral dimensions of the domain are both set to 1 × *LPP*. These spatial settings are selected to ensure adequate room for flow development around the hull and to minimize the influence of boundary effects [22]. The hull model is placed in the domain to simulate steady forward motion in calm water conditions.

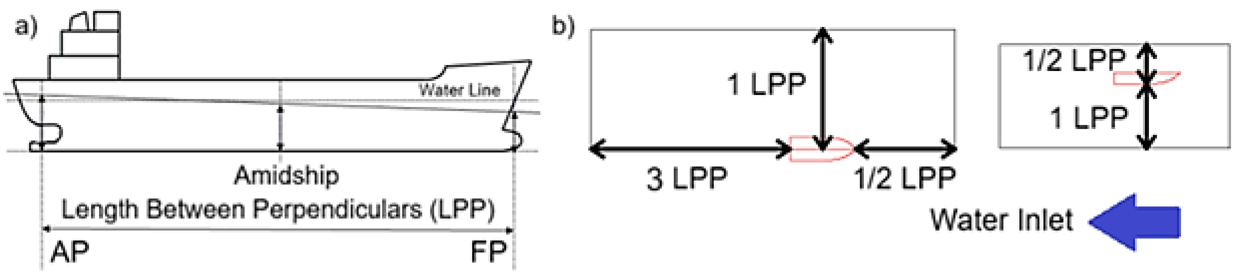

Figure. 4. (a) Illustration of Length Between Perpendiculars (LPP), (b) Boundary Conditions for CFD Simulation Domain.

The discretization of any computational domain into smaller subdomains known as cells is referred to as meshing and those discrete points at the intersection of these elements are called nodes. In CFD, each of the cells acts as a control volume in which the governing equations for the fluid are solved numerically [23].

Mesh quality and density will influence simulation accuracy and convergence character. Finer meshes or those with smaller yet denser cells will, therefore, return more accurate results, capturing the flow gradients as well as the surface geometry better. Less number of cells may have the advantage of low computational expense but would cause a compromise in output accuracy [24]. Therefore, an optimal mesh configuration considers the accuracy-efficiency tradeoff.

Mesh sensitivity analysis is done to evaluate the effect of mesh resolution on numerical accuracy. It is to see how changes in the number of cells (grid density) affect simulation results (i.e. the predicted hydrodynamic resistance) [25].

A. Evaluation Criteria

The evaluation of the hull designs will be carried out by comparing the overall resistance of three different hull configurations at various operational speeds, ranging from 0 to 30 knots [26]. Resistance values for individual speeds will be obtained through CFD simulations, with continued validation using empirical methods such as the Holtrop and Savitsky methods [27].

The Holtrop method is a semi-empirical approach widely adopted for estimating the total resistance of displacement vessels. Developed based on regression analysis of towing tank experiments across a wide range of hull forms, the method offers a reliable resistance prediction with relatively simple inputs. It divides the total resistance R_T into multiple components: frictional resistance R_F, residual resistance R_R, and correlation resistance R_A, each representing different physical phenomena occurring as the ship moves through water. Mathematically, the total resistance is expressed as:

$$R_T = R_F + R_R + R_A \tag{7}$$

where R_R is the resistance due to wave-making and viscous pressure effects, estimated empirically based on hull geometry and speed, R_A is the correction applied to account for differences between model-scale and full-scale results, often expressed as a percentage of R_F, R_F is the resistance primarily caused by viscous effects along the wetted hull surface, calculated using the ITTC-1957 friction line:

$$C_F = \frac{0.075}{(Log10\ Re - 2)^2} \tag{8}$$

where C_F is the frictional resistance coefficient, which represents the resistance caused by water friction along the ship's hull surface, R_e is the Reynolds number, calculated using the formula:

$$R_e = \frac{V \times L_{PP}}{v} \quad (9)$$

where V is the ship's speed in meters per second (m/s), L_{PP} is the characteristic length of the ship, and v is the kinematic viscosity of water, measured in square meters per second (m^2/s).

The frictional resistance force R_F is then calculated as:

$$R_F = C_F \times \frac{1}{2} \times \rho \times V^2 \times S \quad (10)$$

This method is particularly beneficial in preliminary design stages, offering rapid resistance estimation with reasonable accuracy [28].

The CFD verification process consists of two key approaches. The first involves ensuring convergence by minimizing the residuals of the governing equations and keeping them close to zero throughout the simulation. The second approach is a mesh sensitivity analysis, which will be conducted using different cell quantities before the full CFD analysis is performed. For each condition, the independence of resistance results from mesh density will be verified by analyzing resistance at 30 knots [29]. The mesh configuration that produces accurate results with minimal variation across mesh refinements will be selected for the final simulations.

Upon obtaining all resistance data, a comparative evaluation will be conducted by constructing a table that relates hull variation to military functional performance. This table aims to identify the most dominant hull form based on hydrodynamic efficiency and suitability for military applications. Finally, a 3D visual representation of each designed hull will be provided to complement the analysis and support design interpretation.

III. Results and Discussion

A. Hull Geometry Visualization

Before conducting numerical analysis, three distinct hull forms were developed to evaluate their hydrodynamic performance: a conventional V-hull (Model 1), an axe bow hull (Model 2), and a bulbous bow hull (Model 3). These configurations were designed based on standard naval architectural principles, with variations in bow shape intended to improve resistance performance under different operational conditions. The three-dimensional geometries are illustrated in Figure 5, providing a visual comparison of their form characteristics.

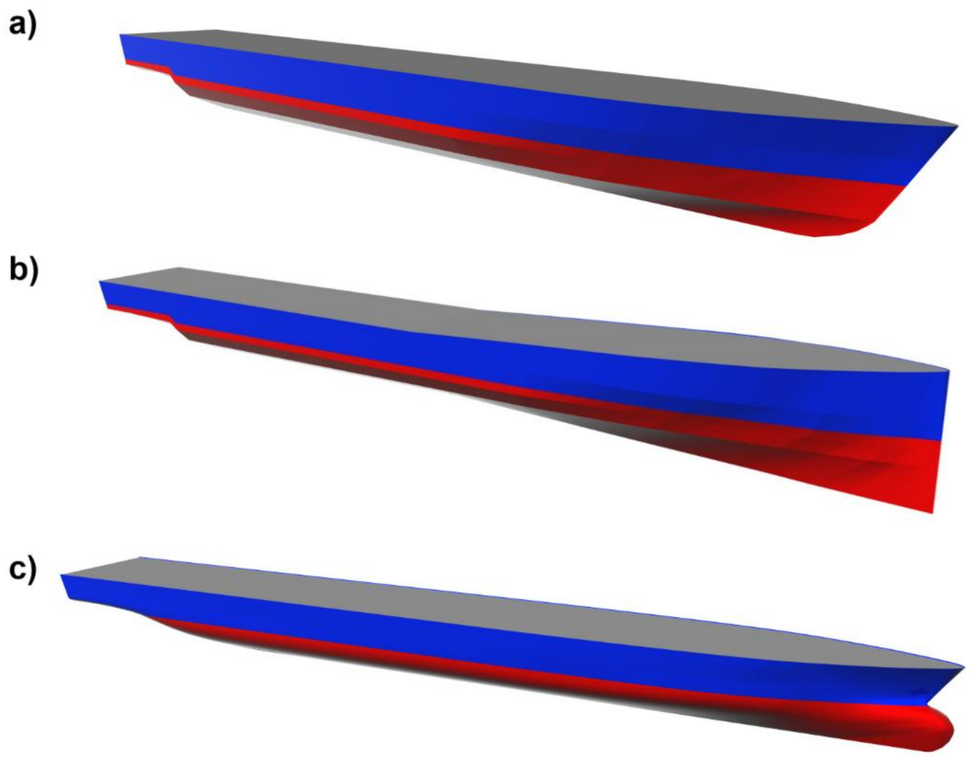

Figure. 5. 3D Geometry of (a) Hull Model 1 (V-Hull), (b) Model 2 (Axe Bow), and (c) Model 3 (Bulbous Bow).

B. Convergence and Mesh Sensitivity Analysis

In numerical simulations, validating solution stability and convergence is essential to ensure result reliability. One key indicator of numerical convergence is the residual value, which quantifies the imbalance in the discretized governing equations at each iteration. A decreasing residual indicates that the iterative solution is approaching the true solution of the equations.

To assess convergence behavior, a residual monitoring process was performed during the simulation of Model 1 at 30 knots. As shown in Figure 6, the residuals experienced significant fluctuations in the early iterations but gradually decreased and reached a steady state after approximately 9,000 iterations. This convergence behavior, with a final residual value of 0.11708795172, indicates that the simulation achieved numerical stability and supports the reliability of the computed resistance results.

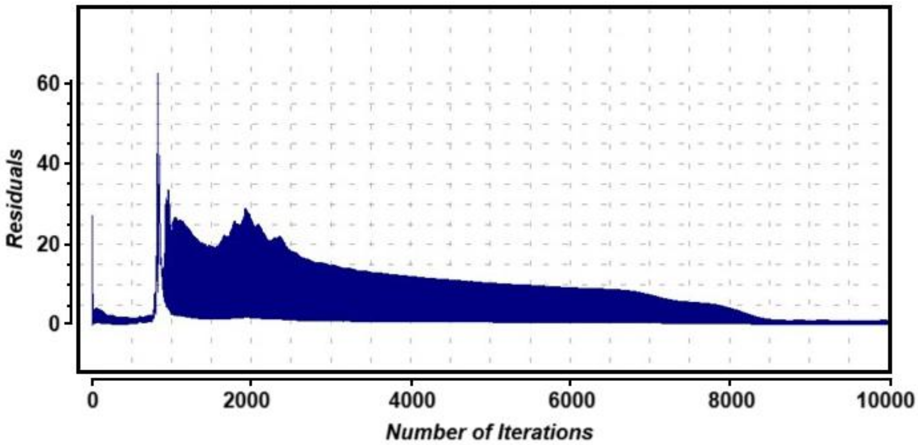

Figure. 6. Residual Convergence Curve for Model 1 Simulation at 30 knots.

The mesh sensitivity analysis was carried for Model 1 by simulating 8 different mesh densities from coarse to fine, with the fine mesh having the total number of cells equal to 3,135,259 and the total resistance of 384.43 kN (Figure 7). The values of total resistance obtained at 30 knots were therefore compared meshes sets (Table 1), the convergence behavior for each simulation was evaluated by monitoring the residual values, which consistently stabilized between 0.2 and 0.8, indicating reliable numerical results without the need for percent error analysis [22].

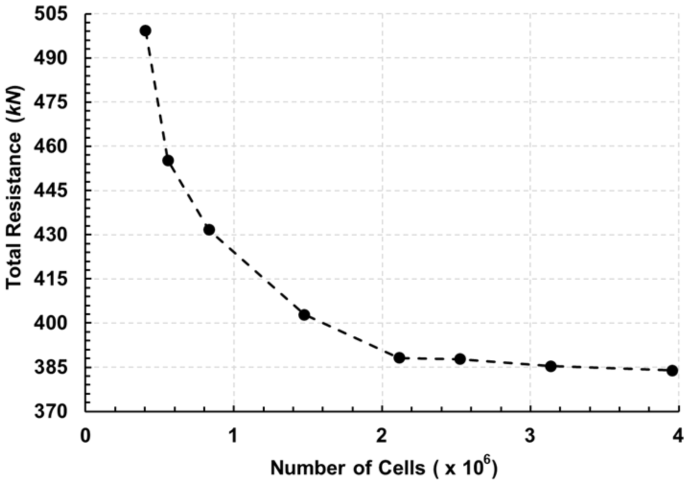

Figure. 7. Total Resistance (R_T) of Model 1 at 30 knots Across Varying Mesh Densities, Showing Convergence Beyond 2 Million Cells.

TABLE 1.
THE TOTAL RESISTANCE (R_T) WAS DETERMINED BY PERFORMING SIMULATIONS WITH PROGRESSIVELY FINER MESH RESOLUTIONS.

Simulation Number	Number of Cells	Total Resistance (kN)	Residual Value from Simulations
1	405324	499.25	0.83783799409
2	555716	455.26	0.69968101720
3	832846	431.68	0.50860835684
4	1475957	402.82	0.35203701257
5	2115148	388.16	0.19992001057
6	2523578	387.74	0.18503299355
7	3135259	385.43	0.11708795172
8	3954938	383.95	0.12806799517

According to Table 1, in the early mesh refinements, total resistance drops very fast from a coarsest mesh of 499.25 kN to approximately 388.16 kN at around 2 million cells. After that, the resistance values change only slightly from the last three simulations, yielding almost identical outputs. This progression affirms the achievement of convergence on mesh, and beyond 3 million cells, accuracy improvement becomes insignificant relative to the computational cost, making the seventh mesh set (3,135,259 cells) a preferable option for further analysis.

C. Analysis Resistance Prediction Using CFD

To evaluate the hydrodynamic performance of the three hull designs, CFD simulations were carried out at vessel speeds ranging from 0 to 30 knots in 5-knot intervals. The total resistance results obtained from each model are presented in Figure 8

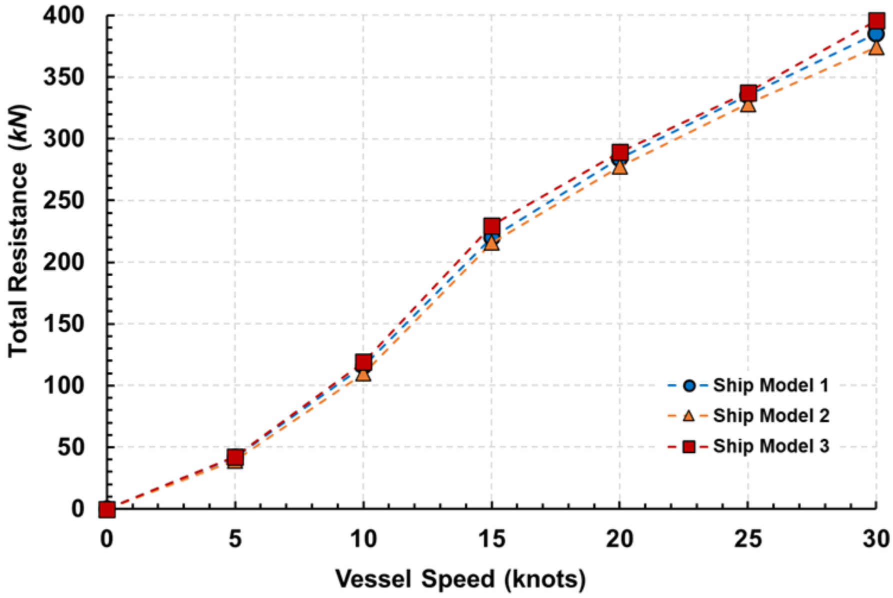

Figure. 8. Total Resistance Versus Vessel Speed for Three Hull Models Based on CFD Simulations.

As shown in the figure, all models display an increasing resistance trend with speed. While resistance values are comparable at lower speeds, notable differences emerge above 20 knots. Among the three designs, Ship Model 2 which features an axe bow consistently shows slightly lower total resistance, particularly at higher speeds. The development that is being observed relates to an axe bow which is vertically slender, wave-piercing geometry, by which the hull cuts through the incoming waves instead of riding on them, this represents a significant advantage in high-speed multihull vessel designs.

McGibbon and Rizvi [30] indicate that around the shore, where reflection of the wave is noticed, the hull has a complex and sometimes contorted attitude: sometimes there is immense pressure, especially in pitch, which is a result of uneven superposition of the incoming waves and the reflected ones; hence, interactions with reflected waves are not necessarily smooth but are highly heading- and frequency-dependent. The high forward sides of the axe bow mitigate deck wetting when plunging down into the waves; however, low buoyancy needs load distribution carefully to avoid trimming. While from the perspective of improving hydrodynamic efficiency, configuration can reduce wave-making resistance under favorable conditions; adverse effects on seakeeping can result because of nearshore reflected-wave conditions unless managed through appropriate heading selection [30].

In line with the findings of McGibbon and Rizvi, Figure 9 presents the wave pattern generated by CFD simulations. The simulation clearly demonstrate the presence of a highly effective wave-piercing zone around the bow region of the hull. The tightly packed contour lines observed at the forward section indicate a steep gradient in wave elevation, which is characteristic of strong pressure differentials generated by the hull as it penetrates the wave field. This observation confirms that wave-making resistance is being minimized.

Additionally, the wave patterns along the sides of the hull appear smooth and symmetrical, with no signs of flow separation or asymmetry, which implies that the flow remains attached along the wetted surface a critical factor in reducing form drag and maintaining pressure recovery.

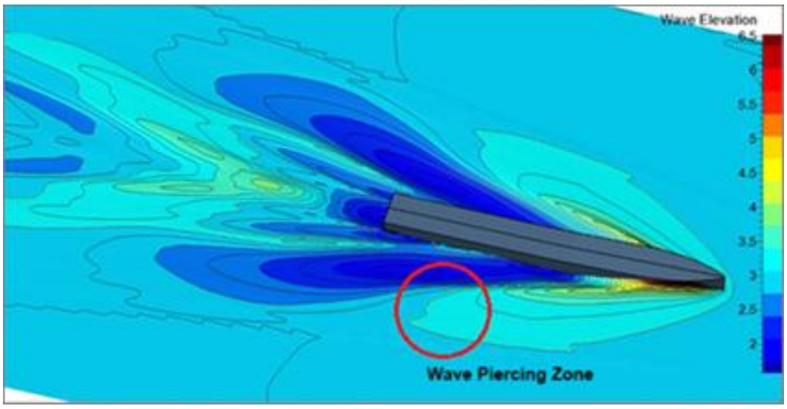

Figure. 9. Wave Elevation Contours Generated by CFD Simulation for an Axe Bow Hull.

D. Empirical Validation

Verifying the results from CFD predictions against multiple reference numerical techniques forms the essential prerequisite for qualifying the simulation setup, boundary conditions, and solver arrangements toward representing reliable results. It is well-established that empirical-based approaches like Holtrop method and Savitsky method have proved extremely handy and have long been used in naval architecture. Benchmark methods provide an opportunity of comparing the level of agreement between CFD outputs and the empirical models, allowing one to quantify how systematic bias occurs. This process not only enhances trust in CFD results but also sheds light on what types of physical phenomena are captured by CFD that may not be adequately modeled by regression or analytical formulas.

Validation of the CFD resistance predictions was carried out at the high speed of 30 knots, where nonlinear wave-making and viscous effects become more pronounced, and empirical methods typically diverge from the more detailed behavior captured by numerical simulations. The results are presented in Table 2.

TABLE 2.
COMPARISON OF RESISTANCE PREDICTIONS AT 30 KNOTS FOR THREE HULL VARIATIONS, WITH DIFFERENCES RELATIVE TO CFD RESULTS.

Variation	Holtrop Resistance (kN)	Savitsky Resistance (kN)	CFD Resistance (kN)	Δ Holtrop – CFD (%)	Δ Savitsky – CFD (%)	Δ Holtrop – Savitsky (%)
Model 1	375,74	329,6	384,43	2,26	14,26	13,99
Model 2	365,18	321,07	374,27	2,42	14,21	13,73
Model 3	368,14	323,17	375,76	2,02	13,99	13,91

The comparison indicates that Holtrop consistently underestimates resistance by approximately 2% relative to CFD, while Savitsky shows a larger underprediction of around 14%. These discrepancies closely match the validation findings reported by Julianto et al., where Holtrop and Savitsky exhibited similar deviation magnitudes when compared to numerical predictions. The alignment of percentage differences confirms that the CFD model in the present work is consistent with established literature trends, further supporting its credibility for high-speed resistance estimation and comparative hull performance analysis [31].

E. Hull Selection Based on Functional Criteria

The hull form selection for a naval vessel must consider not only hydrodynamic efficiency but also its alignment with operational requirements in the designated theater of operation. For patrol and combat missions in the Natuna area, the vessel will encounter varying sea states, including short steep waves caused by monsoon winds and complex coastal interactions. In such conditions, reduced resistance is essential for maintaining high cruising speeds and minimizing fuel consumption, while good seakeeping ensures crew endurance and weapon system stability. Stability at high speed, rapid maneuvering for interception, and the ability to sustain performance in rough seas are critical military functional criteria. To address these factors, a comparative assessment was carried out linking the hydrodynamic performance of each hull variation Axe Bow, Bulbous Bow, and Basic form to its operational suitability for naval missions in the Natuna region. The evaluation focuses on total resistance at 30 knots, stability, seakeeping behavior, and compatibility with mission profiles such as patrolling, interception, and area denial.

TABLE 3.
COMPARISON OF RESISTANCE PREDICTIONS AT 30 KNOTS FOR THREE HULL VARIATIONS, WITH DIFFERENCES RELATIVE TO CFD RESULTS.

Hull Variation	Hydrodynamic Advantages (This Research Focus)	Military Functional Advantages (Other's Researchers Preference)	Reference
Conventional (Model 1)	o Commonly used in warships but has the highest resistance (389.3 kN)	o Higher engine load and fuel consumption compared to other hull forms o Less efficient for high-speed interception and long patrols	[32]
Axe Bow (Model 2)	o Lower total resistance (377.7 kN) o Slender, wave-piercing shape reduces slamming and improves seakeeping o Minimizes turbulence around the bow o More efficient engine performance and reduced fuel consumption	o Low resistance improves ship's operational range and manoeuvrability o Greater endurance due to fuel efficiency o Enhanced agility during target interception o Reduced slamming in rough seas improves weapon system stability	[30][33][34]
Bulbous Bow (Model 3)	o Wave-splitting capability reduces bow wave formation- Lower resistance than conventional hull forms (379.0 kN)	o Reduced pitching and rolling improve crew comfort and mission readiness o Lighter engine load during operation leads to better fuel economy	[35][36]

From the assessment across hydrodynamic and military functional criteria, the axe bow is selected as the preferred hull form for Natuna area warship operations. It combines the lowest resistance at high speed with a wave-piercing geometry that improves seakeeping and reduces slamming, which is critical in the region's variable and often steep coastal waves. The reduced resistance directly translates into better fuel efficiency and extended patrol range, while its slender shape enhances agility and responsiveness during interception tasks. Furthermore, the smoother interaction with waves and minimized turbulence around the bow support more stable platform behavior, benefiting sensors and weapon systems. Although other forms like the bulbous bow offer some comfort advantages and the basic hull is familiar, the overall balance of endurance, speed, maneuverability, and mission versatility makes the axe bow the optimal choice.

F. Visualization of Selected Hull

To support interpretation and facilitate practical implementation, Figures 10, 11, and 12 present the selected Corvette warship hull equipped with the axe bow in three complementary representations. Figure 10 shows the lines plan, detailing the hull geometry in profile, body, and waterline projections to convey the underlying form and curvature. Figure 11 provides the general arrangement, illustrating the overall layout, principal dimensions, and structural organization used in the design. Figure 12 offers a 3D visualization reconstructed from the CAD model and CFD mesh, giving a spatial perspective of the finalized hull shape. Together, these views supply a thorough and coherent geometric description of the adopted hull form, enabling reproduction or integration into downstream design, analysis, or manufacturing workflows.

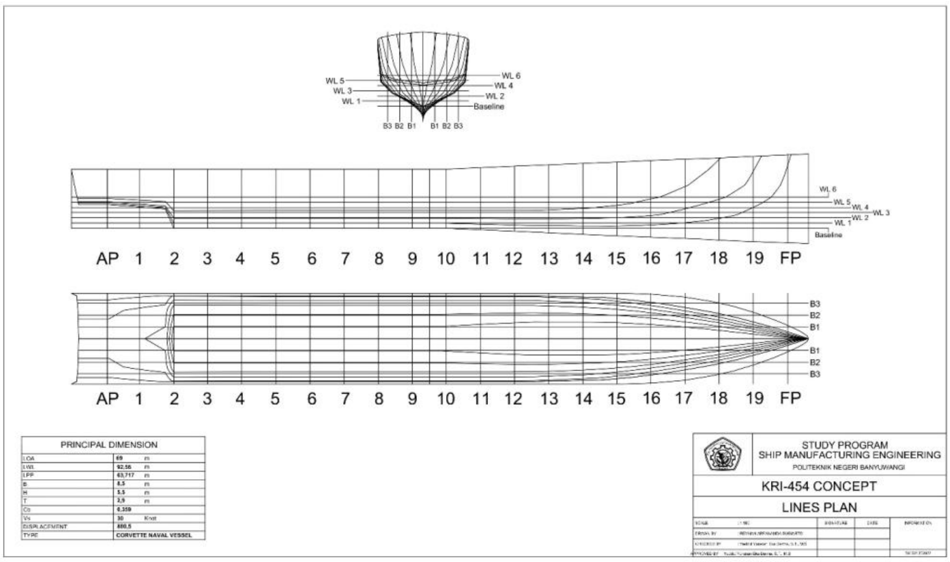

Figure. 10. Lines Plan of the Selected Corvette Warship with Axe Bow Hull Form.

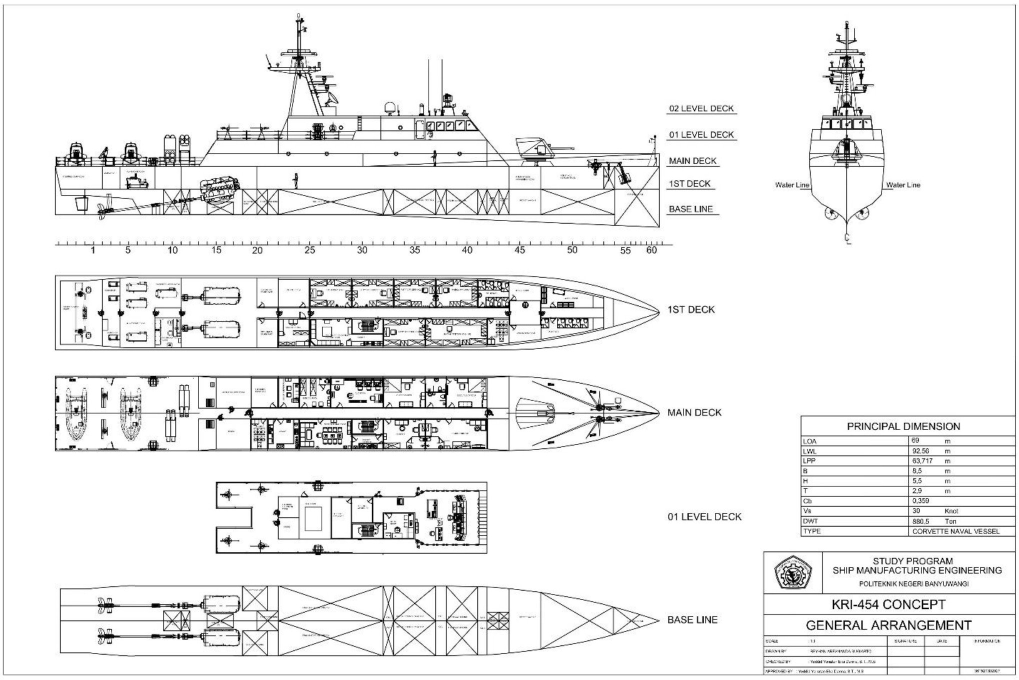

Figure. 11. General Arrangement of the Selected Corvette Warship with Axe Bow Hull Form.

Figure. 12. 3D Visualization of the Selected Corvette Warship with Axe Bow Hull Form.

The primary novelty of this study lies in the identification of the axe bow hull as the most hydrodynamically efficient form for high-speed naval operations in coastal environments. While all hulls show rising resistance with speed, the axe bow consistently outperforms the others above 20 knots, offering tangible benefits in fuel economy and endurance.

IV. Conclusion

This study was conducted to identify the most appropriate hull form for a corvette-class warship operating in the demanding maritime environment of the Natuna Sea. Emphasis was placed on achieving optimal hydrodynamic efficiency and fulfilling operational criteria for high-speed patrol and interception missions. Three bow configurations, a conventional V-hull, bulbous bow, and axe bow were evaluated through validated computational fluid dynamics (CFD) simulations, with additional support from the Holtrop and Savitsky empirical methods.

The results demonstrated that the axe bow configuration consistently achieved the lowest total resistance, particularly at higher speeds, and maintained favourable flow characteristics including attached flow and minimized turbulence. These hydrodynamic benefits translated into superior seakeeping, reduced slamming, and improved propulsion efficiency, as key performance indicators for littoral naval operations. The reliability of the CFD results was confirmed through close agreement with empirical estimates, further supporting the validity of the modelling approach.

While the bulbous and conventional bow forms offered certain advantages, such as comfort and traditional applicability, they did not match the axe bow's comprehensive performance across resistance, and endurance metrics. Accordingly, the axe bow is recommended as the optimal design choice for corvette vessels intended for sustained operations in coastal defence and patrol scenarios.

The future work should focus on advancing this concept toward operational readiness through model-scale experimental validation in towing tanks under conditions representative of the Natuna operational environment.

ACKNOWLEDGEMENTS

The authors would like to express their sincere appreciation to Institut Teknologi Sepuluh Nopember (ITS) for providing the research facilities, computational resources, and technical support necessary to complete this study. Special thanks are extended to the staff and technicians of the Ocean Hydrodynamics Laboratory, Department of Ocean Engineering, for their assistance with CAD modeling, CFD mesh preparation, and simulation execution.

REFERENCES

[1] M. R. Iswardhana, “The Indonesian government responds to protecting the Natuna area through the utilization of national security,” Int. J. Politics Sociol. Res., vol. 12, no. 2, pp. 147–156, 2024.
[2] R. Isak, Z. Fanani, W. Setyo, and D. Tjahjanulin, “Maritime policy integration model at Natuna on the defense and security perspective,” Russ. J. Agric. Socio-Econ. Sci., vol. 100, no. 4, pp. 73–85, 2020.
[3] P. O. Ohwofadjeke, A. E. Udo, and J. O. Jonah, “Characterization of fluid-structure interaction on hydrodynamic performance of different ship hulls using ANSYS,” Comput. Eng. Phys. Model., vol. 7, no. 1, pp. 12–32, 2024.
[4] R. B. Semin and R. Ismail, “Investigation of diesel engine performance based on simulation,” Am. J. Appl. Sci., vol. 5, no. 6, pp. 610–617, 2008.
[5] M. M. H. Bappy and S. R. Hasan, “Enhancing inland vessel efficiency: A comprehensive study on the effectiveness of bulbous bow in mitigating resistance in Bangladesh,” Results Eng., vol. 24, p. 103394, 2024.
[6] A. M. A. El-Ela, M. M. Hussien, and A. M. Elhadad, “Bulbous bow shapes effect on ship characteristics: A review,” in J. Phys.: Conf. Ser., vol. 2811, no. 1, p. 012012, Jul. 2024.
[7] J. L. Gelling, “The axe bow: The shape of ships to come,” in Proc. 19th Int. HISWA Symp. Yacht Des. Yacht Constr., Amsterdam, pp. 1–10, Nov. 2006.
[8] B. Talukdar, “Comparative resistance and seakeeping analyses of warship displacement monohulls, when modified to inverted bow forms from conventional bow,” Tr. Krylov State Res. Cent., no. 2(400), pp. 67–78, 2022.
[9] K. Niklas and H. Pruszko, “Full scale CFD seakeeping simulations for case study ship redesigned from V-shaped bulbous bow to X-bow hull form,” Appl. Ocean Res., vol. 89, pp. 188–201, 2019.
[10] A. P. Kindangen, L. Syahdan, S. Manullang, A. Buwono, and R. Irvana, “Preliminary design of a catamaran ship for water tourism in Lake Sunter,” Int. J. Mar. Eng. Innov. Res., vol. 10, no. 2, 2025.
[11] Lloyd’s Register Rules and Regulations for the Classification of Ships, Volume 1: Ship Structures (Part 5: Ship Design and Construction), Chapter 3: Local Design Loads, Section 1, Lloyd’s Register, London, U.K., 2016.
[12] A. Papanikolaou, Ship Design: Methodologies of Preliminary Design. Cham, Switzerland: Springer, 2014.
[13] A. M. Kracht, Design of Bulbous Bows, SNAME Transactions, vol. 86, pp. 197–217, 1978.
[14] W. Aulia and Y. K. Adi, "Study on resistance and intact stability behavior of patrol boat using axe bow hull form to support surveillance activities in the Indonesia territorial sea," J. Appl. Eng. Sci., vol. 19, no. 3, pp. 825–832, 2021.
[15] W. Froude and E. Froude, The Resistance of Ships, no. 23. Washington, DC, USA: U.S. Government Printing Office, 1888.
[16] E. Petersson, Study of Semi-Empirical Methods for Ship Resistance Calculations. M.S. thesis, Dept. of Shipping and Marine Technology, Chalmers Univ. of Technology, Gothenburg, Sweden, 2020.
[17] R. Ponzini, F. Salvadore, E. Begovic, and C. Bertorello, "Automatic CFD analysis of planing hulls by means of a new web-based application: Usage, experimental data comparison and opportunities," Ocean Eng., vol. 210, p. 107387, 2020.
[18] Z. Ali and G. Bognár, "RANS study of surface roughness effects on ship resistance," J. Nonlinear Complex Data Sci., vol. 25, no. 2, pp. 215–236, 2024.
[19] P. Díaz-Carrasco, S. Croquer, V. Tamimi, J. Lacey, and S. Poncet, "Advances in numerical Reynolds-Averaged Navier–Stokes modelling of wave-structure-seabed interactions and scour," J. Mar. Sci. Eng., vol. 9, no. 6, p. 611, 2021.
[20] Z. Chen and J. Deng, "Data-driven RANS closures for improving mean field calculation of separated flows," Front. Phys., vol. 12, p. 1347657, 2024.
[21] F. Stern, R. V. Wilson, H. W. Coleman, and E. G. Paterson, Verification and Validation of CFD Simulations, no. IIHR407. Iowa City, IA, USA: Iowa Institute of Hydraulic Research, 1999.
[22] A. Firdhaus, I. K. Suastika, K. Kiryanto, and S. Samuel, "Benchmark study of FINE™/Marine CFD code for the calculation of ship resistance," Kapal: J. Ilmu Pengetahuan dan Teknologi Kelautan, vol. 18, no. 2, pp. 111–118, 2021.
[23] C. Dapogny, C. Dobrzynski, and P. Frey, "Three-dimensional adaptive domain remeshing, implicit domain meshing, and applications to free and moving boundary problems," J. Comput. Phys., vol. 262, pp. 358–378, 2014.
[24] A. Katz and V. Sankaran, "Mesh quality effects on the accuracy of CFD solutions on unstructured meshes," J. Comput. Phys., vol. 230, no. 20, pp. 7670–7686, 2011.
[25] Z. Lu, M. H. A. Piro, and M. A. Christon, "Mesh and turbulence model sensitivity analyses of computational fluid dynamic simulations of a 37M CANDU fuel bundle," Nucl. Eng. Technol., vol. 54, no. 11, pp. 4296–4309, 2022.
[26] D. J. Kim, S. Y. Kim, Y. J. You, K. P. Rhee, S. H. Kim, and Y. G. Kim, "Design of high-speed planing hulls for the improvement of resistance and seakeeping performance," Int. J. Nav. Archit. Ocean Eng., vol. 5, no. 1, pp. 161–177, 2013.
[27] H. Islam, M. Ventura, C. G. Soares, M. Tadros, and H. S. Abdelwahab, "Comparison between empirical and CFD based methods for ship resistance and power prediction," in Trends in Maritime Technology and Engineering, pp. 347–357, 2022.
[28] F. Sukas, M. Kantaroglu, and O. K. Kinaci, An Adjoint Numerical/Empirical Approach to Predict the Total Resistance of Ships, J. Nav. Archit. Mar. Technol., vol. 2017, no. 208, pp. 31–44, 2017.
[29] S. Deshpande, P. A. Sundsbø, and S. Das, "Ship resistance analysis using CFD simulations in Flow-3D," 2020.
[30] C. L. McGibbon and M. J. Rizvi, “Effects of nearshore wave reflections on the behaviour of an axe bow trimaran hull,” Ship Technol. Res., vol. 68, no. 3, pp. 179–188, 2021.
[31] R. I. Julianto, A. R. Prabowo, N. Muhayat, T. Putranto, and R. Adiputra, “Investigation of hull design to quantify resistance criteria using Holtrop’s regression-based method and Savitsky’s mathematical model: A study case of fishing vessels,” J. Eng. Sci. Technol., vol. 16, no. 2, pp. 1426–1443, 2021.
[32] H. Schneekluth, Ship Design for Efficiency and Economy, 2nd ed., Oxford, UK: Butterworth-Heinemann, 2011.
[33] A. A. K. Rijkens and A. Mikelic, “The hydrodynamic comparison between a conventional and an Axe Bow frigate hull,” in Proc. Int. Nav. Eng. Conf., vol. 16, no. 31, 2022.
[34] A. Windyandari and A. K. Yusim, “Study on resistance and intact stability behavior of patrol boat using axe bow hull form to support surveillance activities in the Indonesia territorial sea,” J. Appl. Eng. Sci., vol. 19, no. 3, pp. 822–832, 2021, doi: 10.5937/jaes0-29354.
[35] E. Begović, E. Della Valentina, F. Mauro, R. Nabergoj, and B. Rinauro, “The impact of different bow shapes on large yacht comfort,” J. Mar. Sci. Eng., vol. 11, no. 3, Art. no. 495, 2023, doi: 10.3390/jmse11030495.
[36] V. Bertram and H. Schneekluth, Ship Design for Efficiency and Economy, 2nd ed., Oxford, UK: Butterworth-Heinemann, 2011.
[37] H. Schneekluth, Ship Design for Efficiency and Economy, 2nd ed., Oxford, UK: Butterworth-Heinemann, 2011.